

1 Fine scale sampling reveals spatial heterogeneity of rhizosphere microbiome in
2 young *Brachypodium* plants

3
4 Shwetha M. Acharya^{1*}, Mon Oo Yee^{1*}, Spencer Diamond², Peter F. Andeer³, Nameera F. Baig¹, Omolara
5 T. Aladesanmi¹, Trent R. Northen³, Jillian F. Banfield² & Romy Chakraborty¹

6

7

8

9 ¹Department of Ecology, Earth & Environmental Sciences Area, Lawrence Berkeley National Laboratory, Berkeley,
10 California 94720, USA

11 ²Department of Earth and Planetary Science, University of California, Berkeley, California 94720, USA

12 ³Environmental Genomics and Systems Biology Division, Lawrence Berkeley National Laboratory, Berkeley,
13 California 94720, USA

14 *These authors contributed equally to this work

15

16 Competing Interests: The authors declare no competing financial interests.

17

18

19

20

21

22

23 **Abstract**

24 For a deeper and comprehensive understanding of the diversity, composition and function of
25 rhizosphere microbiomes, we need to focus at the scale of individual roots in standardized
26 growth containers. Root exudation patterns are known to vary across distinct parts of the root
27 giving rise to spatially distinct microbial niches. To address this, we analyzed microbial
28 community from two spatially distinct zones of the primary root (the tip vs. the base) in
29 *Brachypodium distachyon*, grown in natural soil using standardized fabricated ecosystems
30 known as EcoFABs as well as in more conventional pot and tubes. 16S rRNA based community
31 analysis showed a stronger rhizosphere effect in the root base vs. bulk soil compared to the root
32 tips vs. bulk soil, resulting in an enrichment of Actinobacteria, Bacteroidetes, Firmicutes and
33 Proteobacteria, few OTUs belonging to less characterized lineages such as Verrucomicrobia and
34 Acidobacteria. While the microbial community distributions are similar across growth
35 containers, the EcoFAB displayed higher replicate reproducibility. Genome-resolved and bulk
36 metagenomics revealed that genes associated with transcriptional regulation, transport of
37 nutrients and catabolic enzymes indicating active metabolism, biofilm formation and root
38 colonization were enriched in root tips. On the other hand, genes associated with nutrient-
39 limitation and environmental stress were prominent in the bulk soil compared to the root tips,
40 implying the presence of easily available, labile carbon and nutrients in the rhizosphere relative
41 to bulk soil. Such insights into the relationships between root structure, exudation and microbial
42 communities are critical for developing understanding of plant-microbe interactions.

43

44 **Keywords:** Rhizosphere, Microbial, Biogeography, Model ecosystem, Metagenomics

45 **1. Introduction**

46 Plants exude 20-40% of their photosynthetically fixed carbon through intact root cells into the
47 surrounding soil [1]. Besides root characteristics, root exudates are a key determinant for
48 development of rhizosphere community. These root exudates containing low-molecular weight
49 organic compounds, and together with mucilage and sloughed off root tissues mainly expelled
50 from root tips, root exudates provide a major source of nutrients for the rhizosphere microbiome
51 [2]. These compounds create a unique environment in the rhizosphere that is physiochemically
52 distinct from the surrounding bulk soil and play a key role in recruiting and selecting relevant
53 beneficial microbes to form a rhizosphere microbiome which is also distinctly differentiated
54 from that of the surrounding bulk soil [3].

55 Root exudation patterns have been shown to vary spatially along the root system, exudates from
56 rapidly dividing root tips differ in composition from exudates released from older sections of the
57 root [4]. While the assembly of microbial community along different parts of roots
58 (biogeography) is considered an important parameter in rhizosphere dynamics, systematic and
59 standardized studies probing this deeper are lacking. Most rhizosphere microbiome studies,
60 where plants are grown in soil, do not compartmentalize the roots based on their morphology but
61 rather based on radial distance from the root axis (rhizosphere, rhizoplane and endosphere). As a
62 result, capturing the effect of spatial differences along the roots is much unexplored, causing a
63 gap in understanding how these differences impact microbial assembly in the rhizoplane.

64 Furthermore, while few studies in the past have demonstrated influence of plant growth
65 container type on plant morphology [5–9], direct impacts of growth containers on the
66 rhizosphere microbiome is relatively unexplored. Complex biochemical processes and
67 interactions occur in microscale dimensions surrounding the root as outlined above. The ability

68 to interrogate these processes within highly reproduceable and controlled growth containers will
69 propel our understanding of rhizosphere spatial heterogeneity [10].

70 In this study, we investigated rhizosphere biogeography from two distinct root zones of
71 *Brachypodium distachyon* grown in natural soil but in three different types of growth containers-
72 conventional pots, tubes as well as specially fabricated EcoFABs [11] to assess (a) microbiome
73 structure and function across root tips, root base and bulk soil; and (b) the suitability of
74 standardized growth containers to study plant-microbe interactions at such finer scales. We also
75 tested these different containers under open or closed environments (encased within secondary
76 containment). The EcoFABs had demonstrated to be of high value in standardized investigations
77 of plant traits and microbiome, and have been shown to reproducibly produce plant phenotypic
78 traits and metabolite production [12], but their applicability to study spatially resolved
79 rhizosphere had been hitherto unexplored. We used long read 16S rRNA amplicon sequencing
80 and shotgun metagenomic sequencing to delineate differences between these diverse containers
81 and distinct root zones (root tips, root base). Metagenomic functional potential unraveled
82 significant differences between root tips and bulk soil.

83

84 **2. Materials and Methods**

85 ***2.1 Soil and plant growth conditions***

86 Soil for plant growth was collected from the south meadow field site at the Angelo Coast Range
87 Reserve in northern California (39° 44' 21.4" N 123° 37' 51.0" W) in August 2020. The upper
88 layer (0-10 cm) was collected in clean collection bags, immediately transported on ice and stored

89 at 4°C until further processing. The collected soil was passed through a 2 mm sieve to remove
90 larger particles like dry roots and rocks prior to use.

91 In this study, we used three types of containers, EcoFAB, test tubes and plastic pots to grow *B.*
92 *distachyon* (Bd21-3 plant line). EcoFABs (n = 11) were fabricated as reported earlier [13] with
93 slight modifications. Briefly, the oval-shaped polydimethylsiloxane (PDMS) cast measuring 7.7
94 cm x 5.7 cm x 0.5 cm (height x width x depth) providing a container volume of 10 mL was held
95 together by metal clamps and screws. Sterile plastic test tubes (n = 14) used to grow plants were
96 10 cm long with a diameter of 1.5 cm, and had a hole drilled at the bottom to drain excess water.
97 The pots (n = 14) used were 10 cm x 10 cm squares with a depth of 10.5 cm, tapered from top to
98 bottom. The volume of soil in test tube and EcoFAB was kept at 15 g each while the pot
99 contained 600 g. The vertical distance between the sown seed to the bottom of the container was
100 8 cm for EcoFAB and 9 cm for both pot and test tube. Except for soil, all components were
101 sterilized by UV sterilization or autoclaving. In addition, approximately half of all containers
102 were kept sterile in closed Microbox containers (Sac O2, Belgium) while others were kept open
103 to the environment.

104 Cold-treated *Brachypodium distachyon* seeds were de-husked, surface-sterilized in 70% ethanol
105 followed by 50% household bleach for 5 minutes each and rinsed thoroughly in sterile water.
106 They were germinated on sterile 0.8% noble agar plates under sunlight at room temperature for
107 two days. Germinated seedlings were transferred into the containers taking care to place it 0.5
108 cm below the soil surface, watered once at 100% capacity with sterile water. Subsequent
109 watering was done at 15% holding capacity, every 2 and 4 days for the open and closed
110 containers respectively. The plants were placed in a greenhouse with a 16-hour photoperiod,

111 87.5% relative humidity, and average day and nighttime temperatures of 19.9 °C and 17.9 °C
112 respectively.

113 ***2.2 Plant phenotypic measurements***

114 Plants were harvested from all containers 14 days after sowing when the primary root had
115 reached bottom of EcoFAB, and key plant phenotypic characteristics were measured. After
116 excising the roots from the base of plant shoot, dry shoot weight was obtained by oven drying the
117 shoots at 80 °C for 24 h followed by cooling to room temperature and measuring dry weight [14–
118 16]. Shoot length was measured from end of the longest leaf to the point where root starts [17].
119 Root length was measured from root base to tip of the primary root.

120 ***2.3 Rhizosphere and bulk soil sample collection***

121 At the time of harvest, roots were excised carefully from soil under aseptic conditions and lightly
122 shaken to remove loosely attached bulk soil. Root tip and root base samples were harvested as 2
123 cm cuttings, measured from tip of the root, and from base of the plant shoot respectively. Due to
124 complications during sampling resulting in physical damage to the roots, some samples were
125 discarded reducing the number of root samples to n = 8, n = 11, and n = 7 originating from
126 EcoFAB, test tube, and pot respectively. The loosely-bound rhizosphere soil was obtained by
127 vortexing the root in 5 mM sodium pyrophosphate for 15 seconds, three times. The root was then
128 placed in fresh pyrophosphate buffer and sonicated for 5 mins to extract tightly-bound fraction.
129 To ensure the complete representation of the rhizosphere microbiome, both the loosely- and
130 tightly-bound fractions were pooled for subsequent DNA extraction. Bulk soil (0.5 g) was
131 collected from containers at least 1 cm away from the roots and kept frozen before DNA
132 extraction.

133 ***2.4 DNA extraction and sequencing***

134 Genomic DNA was extracted using DNeasy PowerLyzer Powersoil kit (Qiagen, US) following
135 the manufacturer's instructions and the eluted genomic DNA was quantified using Qubit™
136 dsDNA High Sensitivity assay kit (ThermoFisher, US).

137 For bacterial full-length 16S rRNA amplification and sequencing, genomic DNA from all the
138 available different root locations and bulk soil were sent to Loop Genomics (US). Briefly, the
139 DNA was amplified with indexed forward (5' CTGCCTAGAACA [Index, F]
140 AGAGTTTGATCMTGGCTCAG 3') and reverse primers (5' TGCCTAGAACAG [Index, R]
141 TACCTTGTTACGACTT 3') and sequenced using the Illumina sequencing platform via paired
142 end (150bp X 2) mode followed by the standard Loop Genomics informatics pipeline that uses
143 short reads to construct synthetic long reads [18].

144 For metagenomic sequencing, replicates of each sample type (root tip, root base or bulk soil from
145 each type of container) was pooled to accommodate the 200 ng DNA concentration requirement,
146 resulting in a total of 9 samples. These samples were sent to QB3-Berkeley Functional Genomics
147 Laboratory (University of California, Berkeley, US) (<http://qb3.berkeley.edu/fgl/>) for library
148 prep and subsequent sequencing using Illumina 150 bp X 2 paired end reads with a depth of 20
149 Gb per sample.

150 ***2.5 16S rRNA community analysis***

151 16S amplicon samples which contained less than 1000 reads after demultiplexing were discarded
152 before analysis. We ensured that there were at least 3 replicate samples for every type of sample
153 under the three variables tested; 1. Container (EcoFAB, pot or test tube), 2. Location (root tip,
154 root base or bulk soil) and 3. Condition (Closed or Open). The demultiplexed data from loop

155 genomics was then clustered into OTUs using usearch (version 11.0.667) for comparative
156 analyses as follows [19]. Briefly, FASTQ files were 1st trimmed (1400 bps) and quality filtered
157 (maximum expected error cutoff 1.0) before initial clustering and chimera filtering using Unoise
158 3 command. The resulting OTUs were further clustered to 97% identity before generating the
159 OTU table, taxonomic assignments and comparative analyses.

160 From the OTUs generated through usearch, DECIPHER v2.0 (r studio package) was used to
161 obtain taxonomic information based on the SILVA SSU version 138 [20, 21] following default
162 parameters. The generated OTU samples were subjected to Hellinger transformation using
163 decostand method in vegan R package version 2.5-7 [22] to standardize differences in
164 sequencing depth prior to diversity analysis. Differential abundance of microbial OTUs across
165 different containers and sample locations were determined using the DESeq2 package (version
166 1.14.1) in R [23]. Pairwise comparison between sample locations coupled to each container was
167 carried out using a full DESeq2 model (design = ~Container_Location + Condition). OTUs
168 showing significant log-fold changes ($p_{adj} < 0.05$) in at least one of these comparisons was further
169 selected and visualized on a phylogenetic tree in iTOL [24]. The log fold-change values were
170 tested for correlation using Spearman's test through custom python script. Afterwards, pairwise
171 comparisons were repeated with a reduced model (design = ~Location + Container + Condition)
172 to study the effect on sample location while controlling container and condition variations. Using
173 the transformed data, homogeneity of multivariate dispersions was analyzed for each sample
174 location in each container using betadisper from vegan R package.

175 ***2.6 Metagenome assembly, annotation, and binning***

176 Shotgun metagenomic sequence for the 9 samples (3 containers * 3 locations) were individually
177 assembled using IDBA-UD v1.1.3 [25] with the parameters: -pre_correction -mink 20 -maxk 150

178 -step 10. Following metagenome assembly, all samples were filtered to remove contigs smaller
179 than 1 kb using pullseq (<https://github.com/bcthomas/pullseq>). Open reading frames were then
180 predicted on all contigs using Prodigal v2.6.3 [26] with the parameters: -m -p meta. KEGG KO
181 annotations were predicted using KofamScan [27] using HMM models from release
182 r02_18_2020 using default options. In cases where multiple HMMs matched a protein above
183 threshold, the HMM with the lowest E-value had its annotation transferred to the protein.

184 Metagenome assemblies were binned into draft genomes using a combination of 4 automated
185 binning methods. Briefly, reads from all 9 samples were mapped to assembled contigs \geq
186 2.5 kbp using Bowtie2, and a differential coverage profile for each contig across all samples
187 was used as input for the following differential coverage binners: MaxBin2, CONCOCT, vamb,
188 and MetaBAT [28–31]. The algorithm DasTool [32], was then used to select the highest quality
189 bins across the 4 binning outputs for each metagenome assembly. Finally, the full genome set
190 across all samples ($n = 146$ genomes) was de-replicated at the species level (Average Nucleotide
191 Identity $\geq 95\%$) using dRep [33] with the following parameters: -p 16 -comp 10 -ms 10000 -sa
192 0.95, resulting in a total of 42 species representative genomes. Species representatives were
193 further selected to have $\geq 60\%$ completeness and $\leq 10\%$ contamination as estimated by checkM
194 [34], this resulted in a final set of 32 species representative genomes meeting the criteria. 16S
195 rRNA sequences were extracted from genomes with ContEst16S tool available online
196 (<https://www.ezbiocloud.net/tools/contest16s>, last accessed on August 17, 2022) [35]. These 16S
197 rRNA sequences were compared with the OTUs obtained from amplicon sequencing using
198 BLAST+ [36] to check for taxonomic consistency.

199 *2.7 Phylogenetic and abundance analysis of genome bins*

200 Phylum level taxonomic assignments of 32 de-replicated genome bins and 1 genome (*P.*
201 *calidifontis* - GCA000015805) included as an outgroup were inferred using GTDB-Tk v1.5.1
202 [37] with reference data version r202; phylogenetic relationships between de-replicated genome
203 bins were inferred using GToTree v1.5.22 based on a set of 25 marker genes, and a phylogenetic
204 tree was produced using FastTree2 [38]. The tree was displayed and rooted in Geneious Prime
205 v2020.2.4. The relative abundance of the 32 genome bins in all samples was assessed by cross
206 mapping reads from each of the 9 samples back to the genome bins using Bowtie2, followed by
207 quantification of coverage of genomes in each sample using coverM
208 (<https://github.com/wwood/CoverM>). Differential abundance of genomes between rhizosphere
209 spatial locations was assessed using the DESeq2 package in R [23]. Detailed version of this
210 section can be found in Supplementary material.

211 ***2.8 Bulk Metagenome Analysis***

212 Phylum level taxonomic composition of bulk metagenomes was assessed directly from raw
213 sample reads using graftM [39] run with a custom ribosomal protein L6 (rpL6) marker database
214 constructed from the r202 release of the GTDB database. Differentially abundant KO genes
215 across the different sample locations were determined using the DESeq2 package (version
216 1.14.1) in R [23]. Pairwise comparison between sample locations was carried out using a reduced
217 DESeq2 model (design = ~Location). Heatmap of differentially abundant genes were plotted in
218 R using the variance stabilized abundance values.

219

220 **3. Results**

221 ***3.1 Container type has minimal impact on plant phenotypic growth***

222 We investigated the spatial biogeography of rhizosphere microbiome of *B. distachyon* grown in
223 model fabricated ecosystems (EcoFABs) in comparison with conventional containers. *B.*
224 *distachyon*, a model grass species for wheat family, was chosen as it produces only one fine
225 primary axile root from the base of the embryo [40] on which the microbial spatial analysis was
226 performed.

227 We measured three major phenotypes of plant growth, i.e., dry shoot weight, shoot length, root
228 length, to determine container impacts on general plant growth. The only significant difference
229 was between plants grown in pots in open vs. closed conditions (**Fig. S1**). The microbox used to
230 maintain sterile condition (closed) was observed to trap a visibly higher amount of moisture
231 inside the box and likely created higher water retention promoting plant growth. Regardless, no
232 other significant difference was detected within or among containers despite differences in
233 container architecture.

234 ***3.2 Location on root is the highest driver of microbial community dissimilarity***

235 We analyzed the rhizosphere microbial community from two different root locations of a 14-day
236 old *B. distachyon* and the bulk soil using full length 16S rRNA obtained using synthetic long
237 read technology. Among the 3674 OTUs obtained after quality filtering, 25 different phyla were
238 identified which corresponded to approximately 80% - 87.5% of all reads among the samples.
239 Microbial relative abundance showed on average a dominance of the bacterial phyla
240 Proteobacteria (22.3%-29.3%), Actinobacteriota (14.2%-23.5%), Acidobacteriota(12.2%-
241 16.5%), Chloroflexi(6.3%-10.1%), Planctomycetota (3.7%-4.7%), Verrucomicrobiota (4.2%-
242 7.4%), Bacteriodota (1.6-4.5%) and Myxococcota (1.9-2.6%) in all samples (**Fig. 1a**).
243 Interestingly, phyla Firmicutes had lower relative abundance in bulk (average -0.4%) compared
244 to root tip and root base samples (average - 2.6%). Microbial diversity was lower in root tip

245 compared to bulk soil ($p < 0.005$, Anova and Tukey) or root base ($p < 0.05$, Anova and Tukey) in
246 all three alpha diversity metrics analyzed (species number, Shannon and inverse Simpson) (**Fig.**
247 **S2**). On the other hand, no significant difference in diversity was observed between root base and
248 bulk soil. When compared between the containers for each sample location, for instance, root tip
249 samples between the three containers, there was no significant difference in microbial diversity
250 ($p > 0.05$, Anova and Tukey) indicating negligible container impact. The same was observed for
251 root base and bulk soil sample locations.

252 Comparative analysis of OTUs between different samples was then carried out to investigate the
253 influence of three parameters tested, i.e., container type, location on root and open or closed
254 condition. Principal Components Analysis (PCA) of the samples showed no clear separation
255 among the two conditions or among the three container types whereas a distinct separation was
256 observed between bulk soil samples compared to root base or root tip (**Fig. 1b**). However, no
257 distinction was seen when comparing root base and root tip based on ordination analysis. This
258 was supported statistically using MANOVA/*adonis* which showed the highest dissimilarity
259 contributed by sample location ($R^2 = 0.10934$, $p = 9.99e-05$) followed by container type
260 ($R^2 = 0.06336$, $p = 0.00069$) but no significant dissimilarity caused by either open or closed
261 conditions ($R^2 = 0.02149$, $p = 0.8119$). Next, we examined whether the homogeneity within
262 samples could be influenced by container type. Overall, the EcoFAB samples exhibited a
263 comparable homogeneity among replicates of the same sample locations compared to the other
264 two conventional containers such as pots and test tubes (**Fig. 1c**).

265 *3.3 Pairwise comparison between sample locations showed the same differentially*
266 *abundant OTUs regardless of container type*

267 The OTUs which showed a statistically significant change in any of the pairwise comparisons,
268 regardless of the containers, were selected and visualized using a neighbor-joining tree (**Fig. 2**).
269 Distinct log-fold changes could be observed for comparisons looking at rhizosphere (root base or
270 root tip) vs bulk soil. Further, analysis with Spearman's correlation coefficient showed that the
271 overall log-fold changes of each OTU were statistically positively correlated in most
272 comparisons regardless of container (**Table S1**), with the only exception being the root tip vs
273 root base changes observed in pot vs test tube ($\rho = -0.02$, $p = 0.78$). In all three comparisons,
274 results from EcoFAB samples were consistent with the others.

275 Using comparisons solely based on sample location, the OTUs could be grouped into three
276 distinct clusters (**Fig. 2b**). The first and smallest cluster showed the OTUs exhibiting significant
277 increase in the rhizosphere (root base or root tip) compared to the bulk soil. Among them are
278 multiple OTUs belonging to *Mucilaginibacter* (Bacteriodota), *Bacillus* (Firmicutes),
279 *Paenibacillus* (Firmicutes), and unclassified Oxalobacteraceae (Gammaproteobacteria). The
280 biggest cluster was for OTUs with a large decrease in the rhizosphere which included the phyla
281 Acidobacteriota, Gemmatimonadota and Chloroflexi. The third cluster contained OTUs with
282 minimal increase or decrease compared within sample locations and contained a mix of phyla.

283 *3.4 Taxonomic analysis from metagenomics shows similar community composition to 16S* 284 *rRNA based amplicon data*

285 Read data from shotgun metagenome samples was directly assessed for bulk taxonomic
286 composition using the ribosomal protein L6 (rpL6) marker gene. The phylum-level relative
287 abundance in all samples showed dominance by the Proteobacteria, Actinobacteriota,
288 Acidobacteriota, Planctomycetota and Verrucomicrobiota (**Fig. S3a**), similar to the 16S rRNA
289 based community composition (**Fig. 1a**). A PCA plot also illustrated a clustering of the bulk soil

290 samples distinctly from the rhizosphere samples as seen earlier in the corresponding 16S
291 amplicon data (**Fig. S3b**). Overall, the metagenomic taxonomy was in correspondence with the
292 16S amplicon data and both types of analysis revealed minimal changes contributed by container
293 differences.

294 ***3.5 Metagenome assembled genomes (MAGs) represent a small fraction of the total reads***

295 Out of the 32 representative MAGs generated from 9 metagenomes after dereplication and
296 quality filtering (**Fig. 3**), 11 MAGs belonged to Actinobacteriota; 6 MAGs from
297 Gammaproteobacteria; 4 MAGs from Acidobacteriota and Alphaproteobacteriota; 3 MAGs each
298 from Chloroflexota; 2 MAGs from Myxococcota and 1 MAG each from Gemmatimonadota and
299 Elusimicrobiota (**Table S6**). As expected in systems with higher diversity, the total coverage of
300 these genomes was rather low, representing ~3% of the read data. 10 MAGs were identified to be
301 differentially abundant across sample locations (**Fig. 3**). It is interesting to note that one
302 Acidobacterial MAG (*Edaphobacter sp.*) had increased abundance in root tip compared to both
303 bulk and base. Members of *Edaphobacter* genus are reported to be associated with
304 ectomycorrhizal fungi and are important in their root colonization [41]. Only 6 MAGs had 16S
305 rRNA and all these sequences had a 97-100% match with OTUs obtained from amplicon
306 sequencing and similar phylogenetic classification.

307 ***3.6 Metagenome analysis reveals metabolic differences between root tip and bulk***

308 5783 unique KEGG orthology groups (KOs) were annotated in the metagenomes, accounting for
309 ~30% of the total proteins predicted in each metagenome. PCA plot of KEGG Orthology (KO)
310 composition of samples indicated that samples cluster by location irrespective of the container
311 type (**Fig. S4**) and hence container parameter was excluded from further DESeq analysis. There
312 were no differentially abundant KOs when root tip was compared to base, in congruence with

313 observations from PCA analysis of OTUs (Section 3.2). Among the 55 differentially abundant
314 KOs identified (**Fig. 4, Table S7**), 27 were enriched in root tip compared to bulk, while other 27
315 were decreased in tip vs. bulk and 2 KOs (one KO shared with decreased tip vs. bulk
316 comparison) increased in bulk over base.

317 KOs involved in different metabolic pathways were over-represented in tip compared to the bulk
318 suggesting an active microbial population utilizing plant-derived compounds. These KOs, which
319 could be broadly categorized as either enzymes, transcriptional regulators or transporters, play a
320 critical role in substrate utilization as well as root colonization. Enzymes encoded were
321 peptidases (*ampS*, *cwlO*), nucleases (*nucS*), kinases (*rsbW*, *fakA*), and other enzymes involved in
322 fatty acid degradation (*acd*), lipid storage (*tgs/wax-dgat*), cell wall synthesis (*tagTUV*), and
323 redox regulation (*gshA*, *fqr*). Transcriptional factors/regulator genes enriched in root tips were
324 involved in regulation of purine catabolism (*pucR*), arabinogalactan biosynthesis (*embR*), biofilm
325 formation (*sigB*) [42], sulfur utilization (*sutR*) and other functions (*tetR*). The enzyme,
326 peptidoglycan DL-endopeptidase encoded by *cwlO*, has been shown to regulate biofilm
327 formation and consequently root colonization in plant-beneficial rhizobacterium *Bacillus*
328 *velezensis* SQR9 [43]. Interestingly, the anti-sigma factor *rsbW* and sigma factor *sigB* were
329 identified as adjacent genes of *sigB* gene cluster and play important roles in stress resistance,
330 biofilm formation and root colonization in *Bacillus cereus* 905 [42]. Transporters involved in
331 acquisition of copper (*ycnJ*), amino acid translocation (*rhtA*), ion transport (*nhaA*), and other
332 nutrients (MFS (*mmr*) and ABC transporters (*mldD/linD*)) were elevated in root tips. 4 other
333 poorly characterized genes and gene involved in oxidative phosphorylation (*qcrC*) were also
334 increased in the root tips over bulk metagenomes.

335 Microbes in the bulk soil do not have ready access to the labile carbon and nitrogen compounds
336 in the exudate and hence may have to invest more in the biosynthesis of machinery for
337 degradation of recalcitrant substrates and nutrient acquisition. Specifically, this involves KOs
338 corresponding to transfer RNA biogenesis (*mnmE/trmE*, *gidA/mnmG*), transcriptional regulation
339 (*rho*, *ada*), ribosome biogenesis (*rlmI*), and sulfur metabolism (*dmsBC*). Genes involved in heme
340 uptake (*exbBD* and *tonB*) [44], nitrogen assimilation/quorum sensing (*rpoN*) [45]
341 lipopolysaccharide export (*lptF*) were also increased in bulk soil. In addition, KOs involved in
342 glycogen synthesis (*glgA*), polysaccharide biosynthesis/export (*wza/gfcE*), maintenance of
343 cellular integrity under acidic stress (*ompA-ompF* porin), production of coenzymes (*pqqL*)
344 involved in free-radical scavenging, regulation of exopolysaccharide production (*hprK*),
345 periplasmic divalent cation tolerance (*cutA*) and osmotic stress genes (*osmY*) may confer
346 resistance to environmental stressors like osmotic stress and desiccation [46, 47] present in bulk
347 soil.

348

349 **4. Discussion**

350 We investigated the utility of EcoFABs as a possible alternative to conventional containers such
351 as pots and tubes in studying the spatial microbial biogeography of the rhizosphere. Although,
352 studies have shown that container design parameters such as size, density, depth can affect root
353 growth and basic plant physiological traits during early developmental stages [5–9], our study in
354 stark contrast, showed that EcoFABs had no significant impact on phenotypic plant growth.
355 While most of these studies looked at container sizes around 50cm³, these studies were
356 performed using woody tree seedlings such as *Pinus sp.* (Pine tree species) and *Quercus sp.* (Oak
357 tree species). Container impacts may not apply to softer wheat plants such as *B. distachyon* to a

358 discernible extent. This emphasizes the importance of using the correct standardized containers
359 to perform accurate study comparisons for the system under investigation.

360 Next, we investigated the impact of microbial community assembly on the root impacted by
361 container differences using both 16S amplicon sequencing and metagenomics. Based on 16S
362 amplicon sequencing results, the microbial community of each location with respect to root
363 showed relatively similar composition across all containers. Differences were observed mostly in
364 root tip or base locations compared to the bulk soil. At root tips, a decrease of bacterial OTU
365 richness and alpha diversity when compared to bulk soil has been previously reported [3, 48].
366 This reduction in microbial diversity in the rhizosphere is commonly observed [49] as the root
367 exudates create a selective environment, recruiting selected microbes from bulk soil. We further
368 observed that even within the rhizosphere, root tips had lower bacterial diversity (richness and
369 evenness) than root base, which concurs with the other studies conducted on *Brachypodium* roots
370 [50, 51]. Root tip environment appears to be more stochastic compared to the root base as the
371 assembly patterns appear to be more deterministic in older parts of the root [49]. This is true in
372 our study as well, there were a higher number of significant OTUs in the comparison of base vs
373 bulk than comparing tip vs bulk (Fig. 2a). Nonetheless, overall correlations show a significantly
374 positive correlation which meant that the rhizosphere effect is already developing at the tip even
375 for 2 week old seedlings of *Brachypodium*. Usually, microbial composition studies tend to occur
376 at later stages of *Brachypodium* growth [50–52] because the plant often takes 30 – 35 days to
377 reach maturity [40]. Our study, however, shows that a rhizosphere effect may be occurring as
378 early as 14 days into the plant growth albeit a weaker impact at the root tips.

379 Only some of the dominant rhizosphere community members such as Gammaproteobacteria and
380 Bacteriodota matched the observations in a previous study with *Brachypodium* rhizosphere [50].

381 Phyla such as *Betaproteobacteria*, which were highly enriched in a previous study with mature
382 plants [50], were neither abundant nor showed enrichment in the rhizosphere. Nonetheless, other
383 rhizosphere enriched groups in this study include Actinobacteria, Acidobacteria and
384 Verrucomicrobia which seems to be more of an effect of the low pH soil characteristic of our
385 field site [53]. Additionally, in that study [50] *Brachypodium* was grown in sand amended soil
386 which could explain the differences. Actinobacteria, for instance, is associated with rhizosphere
387 in soils with high organic content [54, 55]. In another study where fine scale sampling of 4-
388 week-old *Brachypodium* roots was performed, Firmicutes were more abundant in root tips
389 compared to root base, whereas opposite trend was observed for Verrucomicrobia [51]. Phyla
390 such as Actinobacteria, Proteobacteria and Bacteriodota were reported to be enriched in wheat
391 rhizosphere [56]. Thus, in line with prior studies, our data also suggests that a combination of
392 root exudates and edaphic factors are working in tandem to enrich a specific rhizosphere
393 community.

394 Among 150 OTUs which were differentially abundant between different sampling locations, all
395 OTUs belonging to phylum Firmicutes and Bacteriodota were enriched in rhizosphere over bulk
396 soil. These included genera *Bacillus* and *Paenibacillus* (Firmicutes) and *Mucilaginibacter*
397 (Bacteriodota). Members of *Paenibacillus* have been isolated from rhizosphere of wide variety
398 of plants; several of these are capable of fixing-nitrogen [57–59]. Similarly, several
399 *Mucilaginibacter* strains have been isolated from rhizosphere, and a comparative analysis of
400 various strains in this genus highlighted the presence of diverse carbohydrate active enzymes
401 including cellulose-degrading enzymes [60]. Impacts of different *Bacillus* isolates on
402 *Brachypodium* plants have been characterized previously; *Bacillus* isolates can accelerate
403 growth, provide drought protection [61], influence root architecture [61] and can modulate plant

404 hormone homeostasis. Some *Bacillus*, could be classified as r-strategists, which can quickly
405 grow in response to nutrient availability in rhizosphere [51].

406 Majority of differentially abundant OTUs belonging to Gemmatimonodota, Acidobacteria and
407 Verrucomicrobia had reduced abundance in the rhizosphere compared to bulk. These bacterial
408 groups are slow-growing and oligotrophic [62–64], thus more suited to survive in bulk soil away
409 from the nutrient-rich rhizosphere. On the contrary, the OTUs belonging to Actinobacteria,
410 Gammaproteobacteria and Alphaproteobacteria showed no clear trends—OTUs could be either
411 enriched or depleted in the rhizosphere.

412 We observed congruence between taxonomic results obtained by 16S rRNA gene sequencing
413 and metagenomics (rpL6 marker gene), demonstrating reliability of different sequencing
414 methodologies for bacterial profiling (short read Illumina vs. long-read technology).
415 Comparative analysis of metagenomic functional potential between various sampling locations
416 revealed significant differences between root tips and bulk soil. KO genes involved in different
417 metabolic pathways and root colonization were over-represented in tip compared to bulk
418 suggesting an active microbial population capable of utilizing plant-derived exudates and
419 occupying the rhizosphere. KO genes associated with biosynthesis of machinery for degradation
420 of recalcitrant substrates, nutrient acquisition and stress-tolerance were prominent in bulk soil
421 where readily available substrates are scarce in comparison to the vicinity of roots. These
422 findings are consistent with other metagenomic studies comparing rhizosphere vs. bulk soil [65]
423 and also in agreement with the results from 16S amplicon sequencing, where rhizosphere is
424 abundant in fast-growing groups and bacterial assembly in root tips is stochastic, while bulk soil
425 is enriched with groups that are more oligotrophic and adapted to survive in nutrient-limited
426 conditions.

427 We would also like to highlight a few shortcomings of this study. As a result of low DNA yields,
428 samples were pooled for metagenomics which led to low sample numbers. In addition to this,
429 genome-resolved metagenomics yielded fewer genomes making statistical analysis of genome
430 relative abundance and metabolic enrichment analysis difficult. Differences in gene abundance
431 were observed only between root tips and bulk soil, thus differences within rhizosphere
432 compartments (tip vs. base) are unclear which is probably due to sampling of young plants. This
433 is in turn associated with EcoFAB size which limits how long plants could be grown, but can be
434 easily addressed with bigger molds.

435

436 Thus, we have demonstrated the influence of root exudation patterns in shaping microbial
437 communities on different sections of the root in comparison with bulk soil in as young as 14-day
438 old *Brachypodium* plants through 16S rRNA amplicon sequencing and metagenomic analyses.
439 To further probe into the physiology of root-enriched microbes, we will perform high-throughput
440 enrichment of this rhizobiome on known root exudate compounds to create reduced complexity
441 communities. This biogeography study serves as proof of concept for further investigation into
442 high-resolution sampling of rhizosphere to understand biological interactions occurring at finer
443 scales. We are currently working on engineering materials that can be integrated into EcoFABs
444 to enable localized, sub-millimeter scale sampling at different timepoints.

445

446 5. Acknowledgements

447 This research work was funded through the Microbial Community Analysis and Functional
448 Evaluation in Soils (m-CAFEs) Science Focus Area Program at Lawrence Berkeley National

449 Laboratory funded by the U.S. Department of Energy, Office of Science, Office of Biological &
450 Environmental Research Awards DE-AC02-05CH11231.

451

452 6. Competing Interests

453 The authors declare no competing financial interests

454 7. Data Availability Statement

455 The 16S rRNA amplicon sequences and metagenome-assembled genomes generated during the
456 current study are available in the NCBI SRA repository, under the BioProject ID PRJNA902408.
457 The full assemblies for each metagenome sample are publicly available at our in-house analysis
458 platform, ggKbase (<https://ggkbase.berkeley.edu>).

459

460 8. References

461

- 462 1. Pausch J, Kuzyakov Y. Carbon input by roots into the soil: Quantification of
463 rhizodeposition from root to ecosystem scale. *Glob Chang Biol* 2018; **24**: 1–12.
- 464 2. Dennis PG, Miller AJ, Hirsch PR. Are root exudates more important than other sources
465 of rhizodeposits in structuring rhizosphere bacterial communities? *FEMS Microbiol Ecol*
466 2010; **72**: 313–327.
- 467 3. Bulgarelli D, Schlaeppi K, Spaepen S, Ver Loren van Themaat E, Schulze-Lefert P.
468 Structure and functions of the bacterial microbiota of plants. *Annu Rev Plant Biol* 2013;
469 **64**: 807–838.

- 470 4. Aufrecht J, Khalid M, Walton CL, Tate K, Cahill JF, Retterer ST. Hotspots of root-
471 exuded amino acids are created within a rhizosphere-on-a-chip. *Lab Chip* 2022; **22**: 954–
472 963.
- 473 5. Howell KD, Harrington TB. Nursery practices influence seedling morphology, field
474 performance, and cost efficiency of containerized cherrybark oak. *Southern Journal of*
475 *Applied Forestry* 2004; **28**: 152–162.
- 476 6. South DB, Harris SW, Barnett JP, Hains MJ, Gjerstad DH. Effect of container type and
477 seedling size on survival and early height growth of *Pinus palustris* seedlings in Alabama,
478 U.S.A. *Forest Ecology and Management* 2005; **204**: 385–398.
- 479 7. Tsakalimi M, Zagas T, Tsitsoni T, Ganatsas P. Root morphology, stem growth and field
480 performance of seedlings of two mediterranean evergreen oak species raised in different
481 container types. *Plant Soil* 2005; **278**: 85–93.
- 482 8. Kostopoulou P, Radoglou K, Papanastasi OD, Adamidou C. Effect of mini-plug
483 container depth on root and shoot growth of four forest tree species during early
484 developmental stages. *Turkish Journal of Agriculture and Forestry* 2011; 379–390.
- 485 9. Chu X, Wang X, Zhang D, Wu X, Zhou Z. Effects of fertilization and container-type on
486 nutrient uptake and utilization by four subtropical tree seedlings. *Journal of Forestry*
487 *Research* 2020; **31**: 1201–1213.

- 488 10. Yee MO, Kim P, Li Y, Singh AK, Northen TR, Chakraborty R. Specialized plant growth
489 chamber designs to study complex rhizosphere interactions. *Front Microbiol* 2021; **12**:
490 625752.
- 491 11. Zengler K, Hofmockel K, Baliga NS, Behie SW, Bernstein HC, Brown JB, et al.
492 EcoFABs: advancing microbiome science through standardized fabricated ecosystems.
493 *Nat Methods* 2019; **16**: 567–571.
- 494 12. Sasse J, Kant J, Cole BJ, Klein AP, Arsova B, Schlaepfer P, et al. Multilab EcoFAB
495 study shows highly reproducible physiology and depletion of soil metabolites by a model
496 grass. *New Phytol* 2019; **222**: 1149–1160.
- 497 13. Gao J, Sasse J, Lewald KM, Zhalnina K, Cornmesser LT, Duncombe TA, et al.
498 Ecosystem Fabrication (EcoFAB) Protocols for The Construction of Laboratory
499 Ecosystems Designed to Study Plant-microbe Interactions. *J Vis Exp* 2018; e57170.
- 500 14. Barrs HD, Weatherley PE. A Re-Examination of the Relative Turgidity Technique for
501 Estimating Water Deficits in Leaves. *Aust J Biol Sci* 1962; **15**: 413.
- 502 15. Darko E, Végh B, Khalil R, Marček T, Szalai G, Pál M, et al. Metabolic responses of
503 wheat seedlings to osmotic stress induced by various osmolytes under iso-osmotic
504 conditions. *PLoS ONE* 2019; **14**: e0226151.
- 505 16. Mukami A, Ngetich A, Mweu C, Oduor RO, Muthangya M, Mbinda WM. Differential
506 characterization of physiological and biochemical responses during drought stress in
507 finger millet varieties. *Physiol Mol Biol Plants* 2019; **25**: 837–846.

- 508 17. Bresolin APS, Dos Santos RS, Wolter RCD, de Sousa RO, da Maia LC, Costa de
509 Oliveira A. Iron tolerance in rice: an efficient method for performing quick early
510 genotype screening. *BMC Res Notes* 2019; **12**: 361.
- 511 18. Callahan BJ, Grinevich D, Thakur S, Balamotis MA, Yehezkel TB. Ultra-accurate
512 microbial amplicon sequencing with synthetic long reads. *Microbiome* 2021; **9**: 130.
- 513 19. Edgar RC, Flyvbjerg H. Error filtering, pair assembly and error correction for next-
514 generation sequencing reads. *Bioinformatics* 2015; **31**: 3476–3482.
- 515 20. Quast C, Pruesse E, Yilmaz P, Gerken J, Schweer T, Yarza P, et al. The SILVA
516 ribosomal RNA gene database project: improved data processing and web-based tools.
517 *Nucleic Acids Res* 2013; **41**: D590-6.
- 518 21. Wright E S. Using DECIPHER v2.0 to Analyze Big Biological Sequence Data in R. *R J*
519 2016; **8**: 352.
- 520 22. Jari O. vegan: Community Ecology Package. R package version 1.8-5.
521 <http://www.cran.r-project.org> 2007.
- 522 23. Love MI, Huber W, Anders S. Moderated estimation of fold change and dispersion for
523 RNA-seq data with DESeq2. *Genome Biol* 2014; **15**: 550.
- 524 24. Letunic I, Bork P. Interactive Tree Of Life (iTOL) v5: an online tool for phylogenetic
525 tree display and annotation. *Nucleic Acids Res* 2021; **49**: W293–W296.

- 526 25. Peng Y, Leung HCM, Yiu SM, Chin FYL. IDBA-UD: a de novo assembler for single-
527 cell and metagenomic sequencing data with highly uneven depth. *Bioinformatics* 2012;
528 **28**: 1420–1428.
- 529 26. Hyatt D, Chen G-L, Locascio PF, Land ML, Larimer FW, Hauser LJ. Prodigal:
530 prokaryotic gene recognition and translation initiation site identification. *BMC*
531 *Bioinformatics* 2010; **11**: 119.
- 532 27. Aramaki T, Blanc-Mathieu R, Endo H, Ohkubo K, Kanehisa M, Goto S, et al.
533 KofamKOALA: KEGG Ortholog assignment based on profile HMM and adaptive score
534 threshold. *Bioinformatics* 2020; **36**: 2251–2252.
- 535 28. Wu Y-W, Simmons BA, Singer SW. MaxBin 2.0: an automated binning algorithm to
536 recover genomes from multiple metagenomic datasets. *Bioinformatics* 2016; **32**: 605–
537 607.
- 538 29. Alneberg J, Bjarnason BS, de Bruijn I, Schirmer M, Quick J, Ijaz UZ, et al. Binning
539 metagenomic contigs by coverage and composition. *Nat Methods* 2014; **11**: 1144–1146.
- 540 30. Nissen JN, Johansen J, Allesøe RL, Sønderby CK, Armenteros JJA, Grønbech CH, et al.
541 Improved metagenome binning and assembly using deep variational autoencoders. *Nat*
542 *Biotechnol* 2021; **39**: 555–560.
- 543 31. Kang DD, Froula J, Egan R, Wang Z. MetaBAT, an efficient tool for accurately
544 reconstructing single genomes from complex microbial communities. *PeerJ* 2015; **3**:
545 e1165.

- 546 32. Sieber CMK, Probst AJ, Sharrar A, Thomas BC, Hess M, Tringe SG, et al. Recovery of
547 genomes from metagenomes via a dereplication, aggregation and scoring strategy. *Nat*
548 *Microbiol* 2018; **3**: 836–843.
- 549 33. Olm MR, Brown CT, Brooks B, Banfield JF. dRep: a tool for fast and accurate genomic
550 comparisons that enables improved genome recovery from metagenomes through de-
551 replication. *ISME J* 2017; **11**: 2864–2868.
- 552 34. Parks DH, Imelfort M, Skennerton CT, Hugenholtz P, Tyson GW. CheckM: assessing the
553 quality of microbial genomes recovered from isolates, single cells, and metagenomes.
554 *Genome Res* 2015; **25**: 1043–1055.
- 555 35. Lee I, Chalita M, Ha S-M, Na S-I, Yoon S-H, Chun J. ContEst16S: an algorithm that
556 identifies contaminated prokaryotic genomes using 16S RNA gene sequences. *Int J Syst*
557 *Evol Microbiol* 2017; **67**: 2053–2057.
- 558 36. Camacho C, Coulouris G, Avagyan V, Ma N, Papadopoulos J, Bealer K, et al. BLAST+:
559 architecture and applications. *BMC Bioinformatics* 2009; **10**: 421.
- 560 37. Chaumeil P-A, Mussig AJ, Hugenholtz P, Parks DH. GTDB-Tk: a toolkit to classify
561 genomes with the Genome Taxonomy Database. *Bioinformatics* 2019.
- 562 38. Price MN, Dehal PS, Arkin AP. FastTree 2 — approximately maximum-likelihood trees
563 for large alignments. *PLoS ONE* 2010; **5**: e9490.
- 564 39. Boyd JA, Woodcroft BJ, Tyson GW. GraftM: a tool for scalable, phylogenetically
565 informed classification of genes within metagenomes. *Nucleic Acids Res* 2018; **46**: e59.

- 566 40. Watt M, Schneebeil K, Dong P, Wilson IW. The shoot and root growth of *Brachypodium*
567 and its potential as a model for wheat and other cereal crops. *Functional Plant Biol* 2009;
568 **36**: 960.
- 569 41. Yu W-Y, Peng M-H, Wang J-J, Ye W-Y, Li Y-L, Zhang T, et al. Microbial community
570 associated with ectomycorrhizal *Russula* symbiosis and dominated nature areas in
571 southern China. *FEMS Microbiol Lett* 2021; **368**.
- 572 42. Gao T, Li Y, Chai Y, Wang Q, Ding M. SigB regulates stress resistance, glucose
573 starvation, MnSOD production, biofilm formation, and root colonization in *Bacillus*
574 *cereus* 905. *Appl Microbiol Biotechnol* 2021; **105**: 5943–5957.
- 575 43. Li Q, Li Z, Li X, Xia L, Zhou X, Xu Z, et al. FtsEX-CwlO regulates biofilm formation by
576 a plant-beneficial rhizobacterium *Bacillus velezensis* SQR9. *Res Microbiol* 2018; **169**:
577 166–176.
- 578 44. Nienaber A, Hennecke H, Fischer HM. Discovery of a haem uptake system in the soil
579 bacterium *Bradyrhizobium japonicum*. *Mol Microbiol* 2001; **41**: 787–800.
- 580 45. Chuckran PF, Hungate BA, Schwartz E, Dijkstra P. Variation in genomic traits of
581 microbial communities among ecosystems. *FEMS Microbes* 2022; **2**.
- 582 46. Feng S, Qiu Y, Huang Z, Yin Y, Zhang H, Zhu D, et al. The adaptation mechanisms of
583 *Acidithiobacillus caldus* CCTCC M 2018054 to extreme acid stress: Bioleaching
584 performance, physiology, and transcriptomics. *Environ Res* 2021; **199**: 111341.

- 585 47. Dsouza M, Taylor MW, Turner SJ, Aislabie J. Genomic and phenotypic insights into the
586 ecology of *Arthrobacter* from Antarctic soils. *BMC Genomics* 2015; **16**: 36.
- 587 48. Shi S, Nuccio EE, Shi ZJ, He Z, Zhou J, Firestone MK. The interconnected rhizosphere:
588 High network complexity dominates rhizosphere assemblages. *Ecol Lett* 2016; **19**: 926–
589 936.
- 590 49. Ruger L, Feng K, Dumack K, Freudenthal J, Chen Y, Sun R, et al. Assembly Patterns of
591 the Rhizosphere Microbiome Along the Longitudinal Root Axis of Maize (*Zea mays* L.).
592 *Front Microbiol* 2021; **12**: 614501.
- 593 50. Kawasaki A, Donn S, Ryan PR, Mathesius U, Devilla R, Jones A, et al. Microbiome and
594 Exudates of the Root and Rhizosphere of *Brachypodium distachyon*, a Model for Wheat.
595 *PLoS ONE* 2016; **11**: e0164533.
- 596 51. Wei S, Jacquiod S, Philippot L, Blouin M, Sørensen SJ. Spatial analysis of the root
597 system coupled to microbial community inoculation shed light on rhizosphere bacterial
598 community assembly. *Biol Fertil Soils* 2021; **57**: 973–989.
- 599 52. Donn S, Kawasaki A, Delroy B, Chochois V, Watt M, Powell JR. Root type is not an
600 important driver of mycorrhizal colonisation in *Brachypodium distachyon*. *Pedobiologia*
601 2017.
- 602 53. Diamond S, Andeer PF, Li Z, Crits-Christoph A, Burstein D, Anantharaman K, et al.
603 Mediterranean grassland soil C-N compound turnover is dependent on rainfall and depth,

- 604 and is mediated by genomically divergent microorganisms. *Nat Microbiol* 2019; **4**: 1356–
605 1367.
- 606 54. Tkacz A, Cheema J, Chandra G, Grant A, Poole PS. Stability and succession of the
607 rhizosphere microbiota depends upon plant type and soil composition. *ISME J* 2015; **9**:
608 2349–2359.
- 609 55. Kopecky J, Kyselkova M, Omelka M, Cermak L, Novotna J, Grundmann GL, et al.
610 Actinobacterial community dominated by a distinct clade in acidic soil of a waterlogged
611 deciduous forest. *FEMS Microbiol Ecol* 2011; **78**: 386–394.
- 612 56. Donn S, Kirkegaard JA, Perera G, Richardson AE, Watt M. Evolution of bacterial
613 communities in the wheat crop rhizosphere. *Environ Microbiol* 2015; **17**: 610–621.
- 614 57. Ripa FA, Tong S, Cao W-D, Wang ET, Wang T, Liu HC, et al. *Paenibacillus rhizophilus*
615 sp. nov., a nitrogen-fixing bacterium isolated from the rhizosphere of wheat (*Triticum*
616 *aestivum* L.). *Int J Syst Evol Microbiol* 2019; **69**: 3689–3695.
- 617 58. Kämpfer P, Busse H-J, McInroy JA, Clermont D, Criscuolo A, Glaeser SP. *Paenibacillus*
618 *allorhizosphaerae* sp. nov., from soil of the rhizosphere of *Zea mays*. *Int J Syst Evol*
619 *Microbiol* 2021; **71**.
- 620 59. Li Y, Li Q, Chen S. Diazotroph *Paenibacillus triticisoli* BJ-18 Drives the Variation in
621 Bacterial, Diazotrophic and Fungal Communities in the Rhizosphere and Root/Shoot
622 Endosphere of Maize. *Int J Mol Sci* 2021; **22**.

- 623 60. Wang ZY, Wang RX, Zhou JS, Cheng JF, Li YH. An assessment of the genomics,
624 comparative genomics and cellulose degradation potential of *Mucilaginibacter*
625 *polytrichastri* strain RG4-7. *Bioresour Technol* 2020; **297**: 122389.
- 626 61. Gagné-Bourque F, Mayer BF, Charron J-B, Vali H, Bertrand A, Jabaji S. Accelerated
627 Growth Rate and Increased Drought Stress Resilience of the Model Grass *Brachypodium*
628 *distachyon* Colonized by *Bacillus subtilis* B26. *PLoS ONE* 2015; **10**: e0130456.
- 629 62. Pascault N, Ranjard L, Kaisermann A, Bachar D, Christen R, Terrat S, et al. Stimulation
630 of different functional groups of bacteria by various plant residues as a driver of soil
631 priming effect. *Ecosystems* 2013; **16**: 810–822.
- 632 63. Barber NA, Chantos-Davidson KM, Amel Peralta R, Sherwood JP, Swingley WD. Soil
633 microbial community composition in tallgrass prairie restorations converge with remnants
634 across a 27-year chronosequence. *Environ Microbiol* 2017; **19**: 3118–3131.
- 635 64. Vieira S, Sikorski J, Dietz S, Herz K, Schrumpf M, Bruelheide H, et al. Drivers of the
636 composition of active rhizosphere bacterial communities in temperate grasslands. *ISME J*
637 2020; **14**: 463–475.
- 638 65. Xu J, Zhang Y, Zhang P, Trivedi P, Riera N, Wang Y, et al. The structure and function of
639 the global citrus rhizosphere microbiome. *Nat Commun* 2018; **9**: 4894.
- 640
641
642
643

644

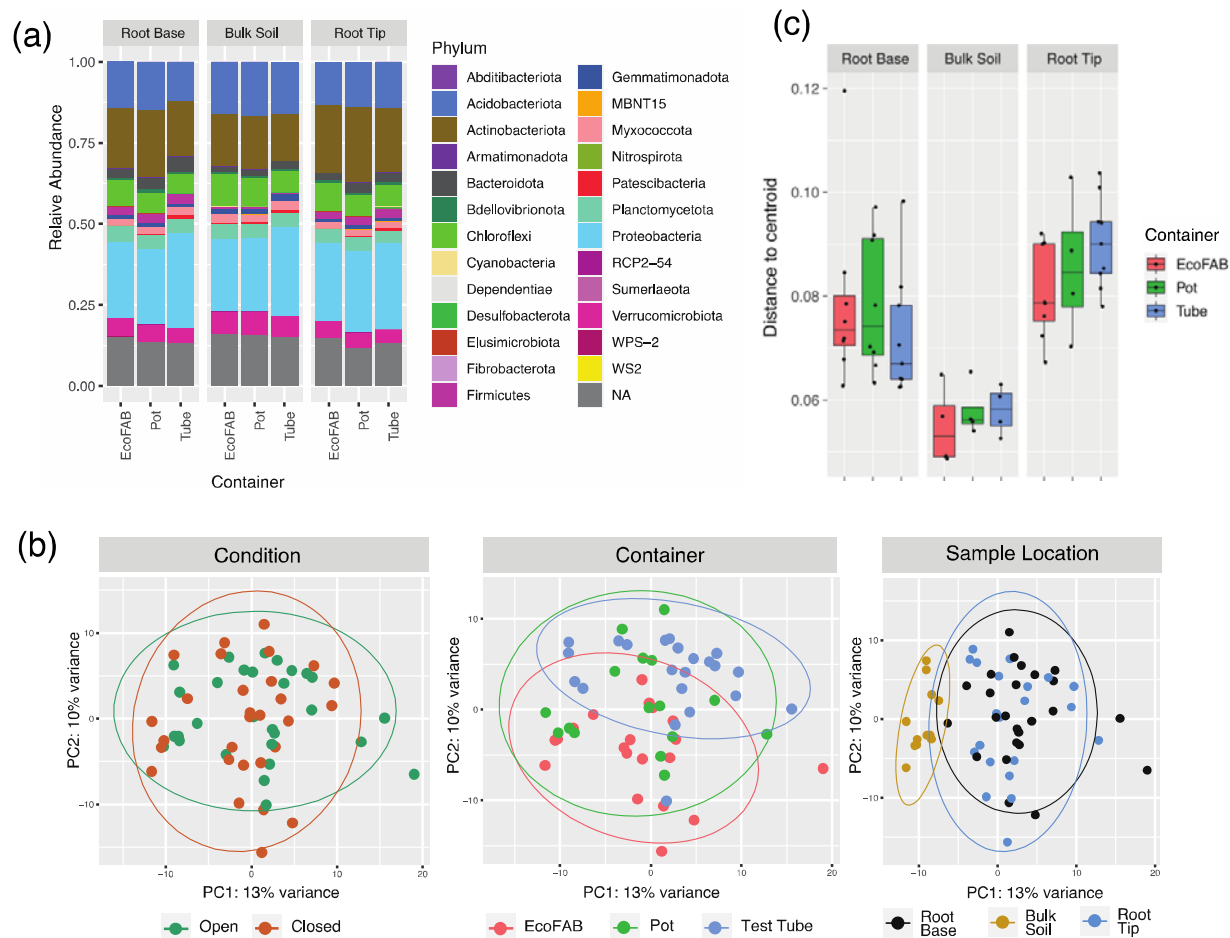
645

646

647

648

649 9. Figures

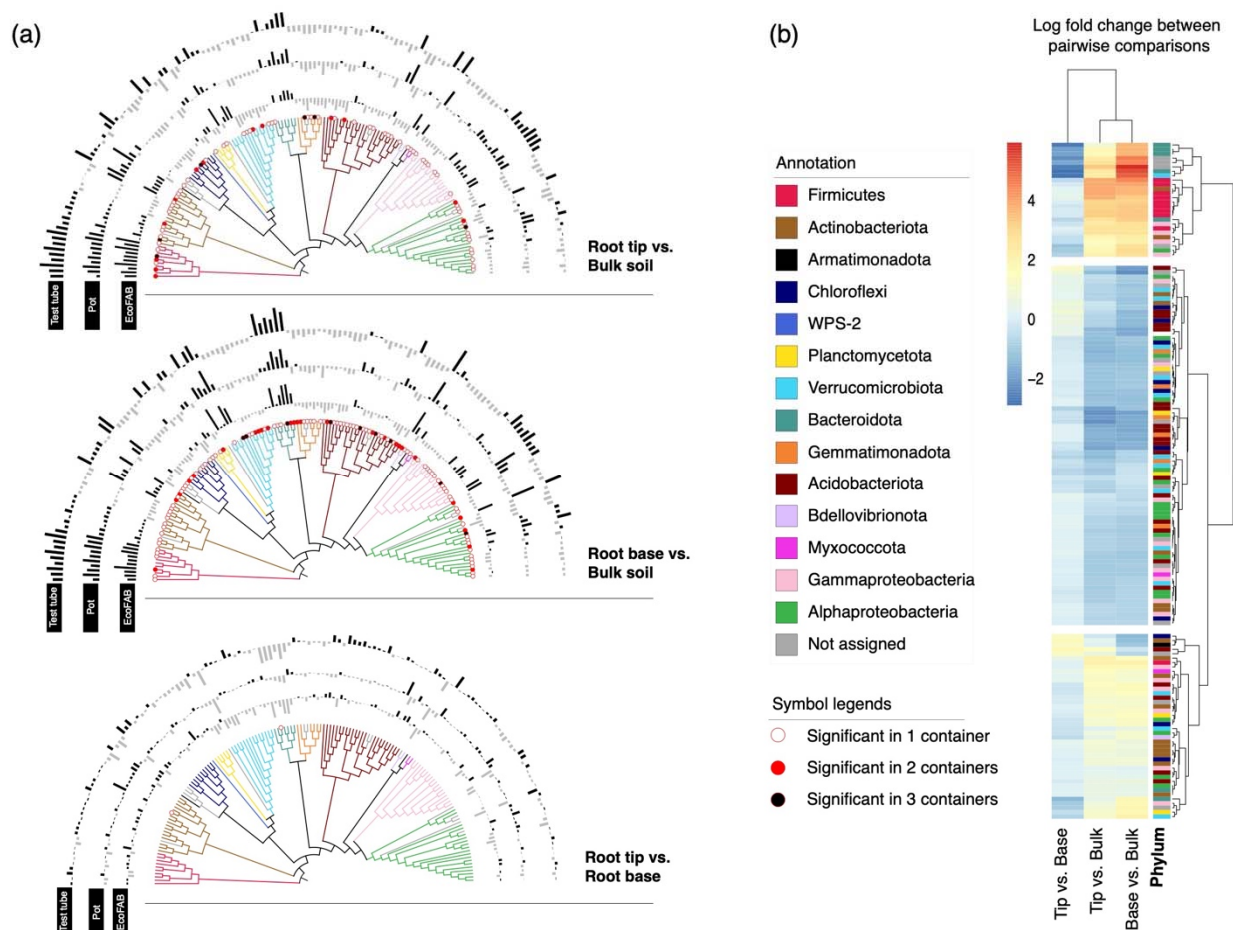


650

651 **Figure 1.** (a) Microbial relative abundance based on 16s rRNA amplicon sequencing of rhizosphere (root

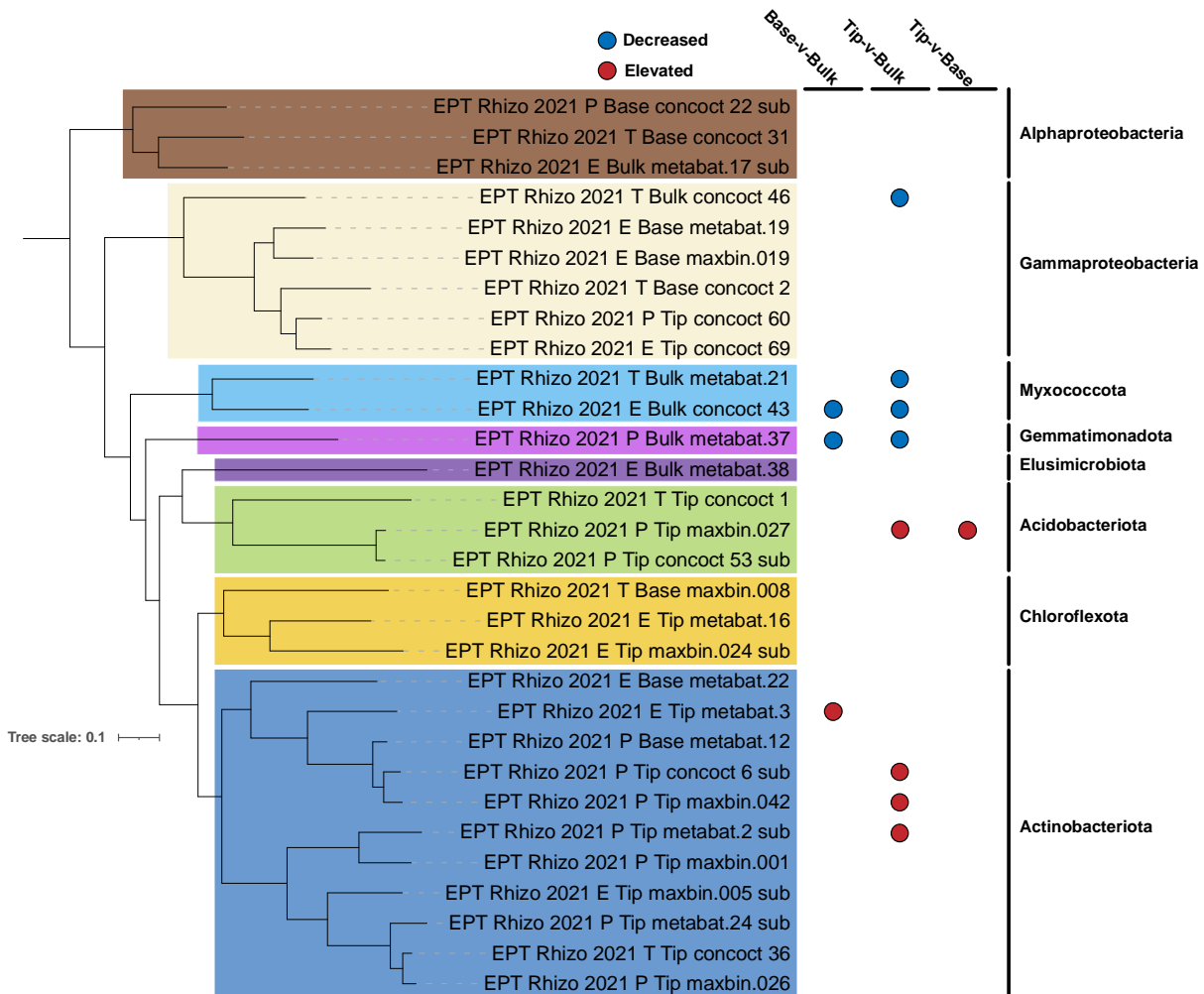
652 tip and root base) and bulk soil samples 14-day old *Brachypodium distachyon* grown in three different

653 containers: EcoFAB, pot and test tubes, (b) PCA plot of variance stabilized 16S amplicon data, the
 654 samples are then visualized according to the three different variables examined: condition, container or
 655 sample location, (c) Boxplot showing multivariate homogeneity of group dispersions grouped according
 656 to sample location and container.



657
 658 **Figure 2.** (a) Neighbor joining tree of selected OTUs which showed significant log fold changes during
 659 pairwise analysis of sample locations. The top tree depicts a pairwise comparison between root tip and
 660 root base and the bottom tree depicts the comparison between root base and bulk soil. The bar chart
 661 around the tree corresponds to log fold changes for each OTU in each of the different containers - test
 662 tube, pot or EcoFAB. An outward bar away from the tree represents a positive log fold change in the and
 663 an inward bar towards the tree represents a negative fold change in the respective OTU. The significant
 664 changes are indicated at the bottom of each node with a symbol. No symbol at the bottom of the node

665 means the fold change is not statistically significant. (b) Clustering of selected OTUs based on pairwise
 666 comparison between sampling locations (ignoring containers) reveals three different clusters. Each OTU
 667 is colored by the phylum it belongs to.
 668



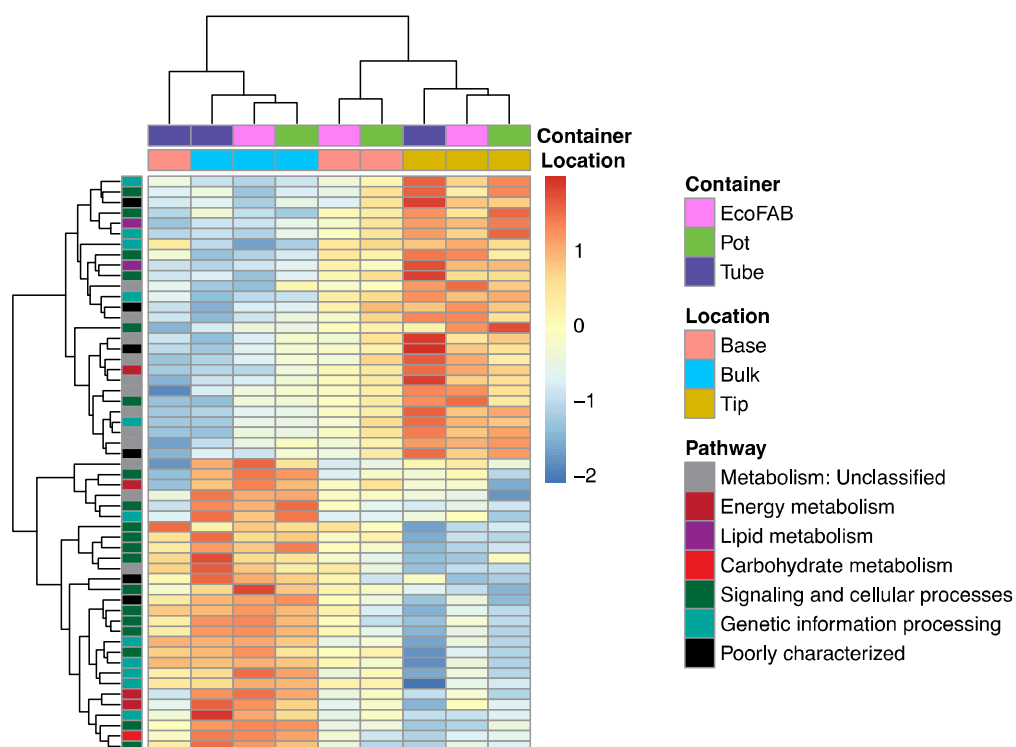
669
 670 **Figure 3.** Phylogenetic tree of 30 of 32 dereplicated MAGs passing tree building criteria (*P. calidifontis* -
 671 GCA000015805 included as outgroup for rooting; not displayed) along with their differential abundance
 672 (significantly elevated or decreased; Wald Test - $FDR \leq 0.05$) based on sample location. MAG names are
 673 colored based on their phylum-level classification and phyla names displayed on the right. Tree was
 674 inferred using a set of 25 phylogenetically informative marker genes conserved between Archaea and
 675 Bacteria.

676

677

678

679



680

681 **Figure 4.** Heatmap of abundance of 55 differentially abundant KEGG Orthology genes across different

682 locations in the 9 metagenome samples based on DESeq analysis (corrected p-value <0.1), normalized by

683 z-score across all datasets. Each row represents a gene, colored by its KEGG level I classification. 27

684 KOs were enriched in root tip compared to bulk, 27 KOs were enriched in bulk compared to tip and 2

685 KOs in bulk over base.

686

687

688

689